

MOBILITY, RECOMBINATION KINETICS, AND SOLAR CELL PERFORMANCE

C. M. Fortmann and D. Fischer, Institut de Microtechnique,
Université de Neuchâtel, 2000 Neuchâtel,
Switzerland, phone +41 38 20 51 21, fax +41 38 25 42 76

ABSTRACT

In order to optimize the amorphous silicon structure for improved stabilized performance it is necessary to understand a great number of material parameters as they exist in the solar cell under operating conditions. Towards the goal of using the solar cells themselves for quantitative defect analysis we show that the short wavelength quantum efficiency measurement is a means to determine the total density of charged and uncharged dangling bonds in the i-layer as a function of light soaking time. The compound effect that dangling bond defects have on solar cell performance, consisting of the redistribution of the electric fields and decreased lifetimes are considered. The magnitude of the short wavelength response can be directly linked to the number of bulk defects in the solar cells. Also it is not possible to directly determine the electron mobility from solar cell characterization due to the diffusive carrier transport found in amorphous materials. Surprisingly, we do expect the electron mobility to be directly linked to the stability of the solar cells.

INTRODUCTION

The material parameters as well as the range of values that can be obtained for materials in the amorphous silicon system have been under study for a number of years. While considerable progress has been made not all of the parameters are known. For example, only recently has the electron mobility been established as a function of deposition condition in i-layer materials.

The development of techniques to extract material parameters from solar cell measurements would open a parallel path by which to determine the materials parameters as well as permit the numerical modeler to obtain the information he needs from the materials as they exist in the solar cell itself. For a variety of reasons these material parameters may be different in the solar cell compared to those found in films. For example, differences between film and solar cell values could arise because of the different Fermi level positions or because some inter-diffusion of species occurred during the deposition of the solar cell. *

The need to extract material parameters from solar cell measurements has motivated the development of a number of techniques. These techniques include the use of thermal carrier generation, primary photo current, and short wavelength quantum efficiency. Recently, it has become apparent that some of these measurements are not unambiguous measurements of bulk defect concentrations. It was recently reported that the failure of the thermal currents to scale with the applied voltage in the manner consistent with bulk defects was due to an interface component [1]. Likewise, the primary photo current was [2] found to not

scale with either i-layer thickness or material quality in manner consistent with bulk defects. Only the change in short quantum efficiency has been shown to scale with i-layer thickness and applied voltage bias in a manner consistent with bulk defects.

The previous analysis [3] of short wavelength quantum efficiency was based on analytical modelling which cannot account for all of the effects that occur in the solar cell i-layer as a function of defect concentrations. These effects include position dependant lifetime changes, field redistribution due to charged defects and changes in the electron back diffusion and loss at the p/i interface [4]. This work will show that despite these complexities the short wavelength quantum efficiency remains an accurate and viable tool for the extraction of defect concentrations that control the lifetime and the charged defect concentrations that distort the electric field.

In this work we will also use the analysis techniques developed (short wavelength spectral response) to consider the rather difficult question of the relationship between solar cell stability and deposition conditions. A number of researchers [5,6] have reported that increased micro-structure in the i-layer materials used for solar cell fabrication have a deleterious effect on the stability of the solar cells. However the saturated defect density in films is a weak function of deposition condition and micro-structure [7].

Attempts to resolve these stability issues in terms of lifetime changes alone quickly lead to contradictions. Therefore, in this work we will place a larger emphasis on the electron mobility which has been recently reported to be a function of deposition conditions and micro-structure [8].

We know from previous numerical modelling work [9] that the changes caused by different electron mobilities do not influence the performance of annealed p-i-n solar cells. The lack of sensitivity to electron mobility in annealed solar cells results from dispersive transport considerations, which predict that a decrease in carrier mobility will result in an increased carrier density. However the recombination rate does not increase because the diffusive velocity is reduced in proportion to the mobility. The lack of mobility dependence in the annealed state however can not be taken as an indication of the relative stability of solar cells since the stability may be related to the carrier densities present in the films during the degradation [10].

METHODS

The solar cells were deposited by VHF glow discharge at 70 MHz. The i-layer thickness is varied from 0.5 to 2 μm . SiC alloy is used as p-layer, material $\mu\text{c-Si:H}$ as n-layer material. No interface buffer layers are employed. One sun light-soaking is performed with a sodium vapor light-source, accelerated light-soaking is performed under red light

illumination at an intensity of 10 suns. The QE is measured with chopped light at an approximate photon flux of $10^{15} \text{ s}^{-1} \text{ cm}^{-2}$. The numerical modelling is based on a model described earlier [11]. Its main features are the use of a defect model with a single level of amphoteric mid-gap defects, and the fixture of the boundary conditions at the doped/intrinsic layer interfaces, avoiding the need to introduce a large number of only vaguely known doped- and interface-layer parameters. By this simplified approach the number of modelling parameters can be kept relatively small.

In the present work, besides absolute QE data often also normalized QE data is plotted. This normalized QE represents the absolute QE (at 0V) normalized with respect to the QE measured at a high reverse bias voltage where a complete collection of the photo-carriers from the whole i-layer can be assumed. Thereby the changes of the collection can be presented free of the distortions of the optical envelope, on a scale from 0 to 1.

RESULTS AND DISCUSSION

The marked drop in non-light biased short wavelength quantum efficiency measurement of degraded p-i-n solar cells has been treated in a number of recent publications. In one view this effect was interpreted as an increase in the surface recombination resulting from light-soaking [12], while

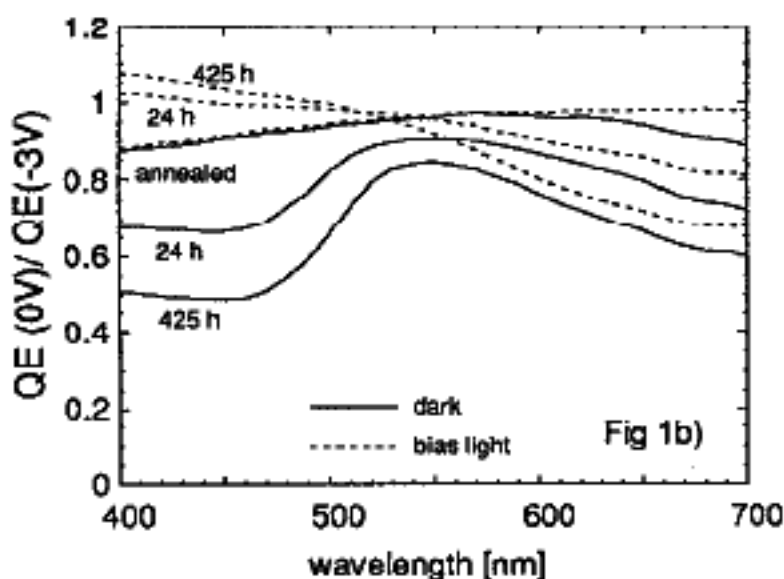
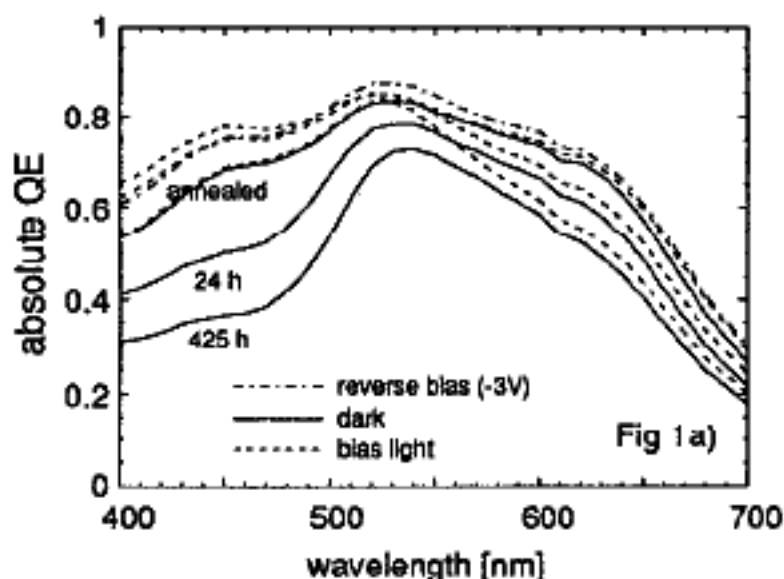


Figure 1: Absolute and normalized spectral response of a p-i-n solar cell with a $0.5 \mu\text{m}$ thick i-layer, in the annealed state, and after 24 and 425 hours of one sun light-soaking.

elsewhere the effect was related to bulk defects [3,4]. Consistent with the bulk defect interpretation are the observations that the reduction of the short wavelength QE scales with the solar cell i-layer thickness and with light-soaking time [3].

Only recently have advanced numerical models been applied to obtain a quantitative determination of the factors that influence the short wavelength quantum efficiency. The factors that the computer models can take into consideration include chargeable mid-gap defects, and the self consistent solution of the electron and hole continuity equations and poisson's equation. These models show that the drop in blue response (without light bias) is due to a self blocking effect of the electrons [4,13]: caused by the negative charging of the mid-gap defects. These negatively charged defects cause a reduction of the electric field strength at the p-i interface leading not only to an accumulation of electrons in the front part of the i-layer but to enhanced hole back-diffusion into the i-layer. The electron accumulation and hole back diffusion lead directly to increased recombination losses.

Figure 1 shows the QE with and without bias light of a p-i-n cell with an i-layer thickness of $0.5 \mu\text{m}$ for different light-soaking times (Fig 1a: absolute QE, Fig 1b: relative QE). The short wavelength QE in the dark, which is high in the initial state, is shown to continuously decay with increasing light-soaking time, whereas the short wavelength QE with bias light remains closed to the complete collection case found in annealed solar cells. The short wavelength QE drop in the dark is the result of the self-blocking effect of the electron transport in the non illuminated solar cell as discussed above. The amplitude of the change is larger than the drop in the red response. Red response is independent of the bias light conditions. Yet, it is important to point out that this marked loss of the short wavelength response only occurs under the particular condition of illumination with short wavelength light without bias light and does therefore not indicate an actual solar cell loss mechanism, as in an operating solar cell the necessary bias light is supplied by the AM1.5 spectrum. The drop of the short wavelength response in the dark can thus not be used as supporting evidence for an interface degradation model as it was done previously [12]. The reduced red light collection is independent of the bias light and therefore represents an actual loss mechanism indicating reduced collection from areas remote from the p-i interface [11].

The symbols in Figure 2 show the experimental dark QE at 450 nm (QE_{450}) of p-i-n solar cells as a function of the i-layer thickness, before and after high intensity light-soaking. In the annealed state, the QE_{450} in the dark is closed to full collection of the over the whole observed i-layer

Table I: Parameters for the numerical modelling

Mobility gap [eV]	1.8
Built in potential [V]	1.1
Electron conc. at n-i interface [cm^{-3}]	$1 \cdot 10^{16}$
Surface rec. velocity p-i interface [cm s^{-1}]	$3 \cdot 10^4 \dots 3 \cdot 10^5$
Hole conc. at p-i interface [cm^{-3}]	$1 \cdot 10^{14}$
Surface rec. velocity n-i interface [cm s^{-1}]	$1 \cdot 10^4$
Electron mobility [$\text{cm}^2 \text{V}^{-1} \text{s}^{-1}$]	10
Hole mobility [$\text{cm}^2 \text{V}^{-1} \text{s}^{-1}$]	1
Mid-gap defect density [cm^{-3}]	$1 \cdot 10^{15} \dots 3 \cdot 10^{16}$
x-section neutral defects [cm^2]	$3 \cdot 10^{-16}$
x-section charged defects [cm^2]	$3 \cdot 10^{-15}$

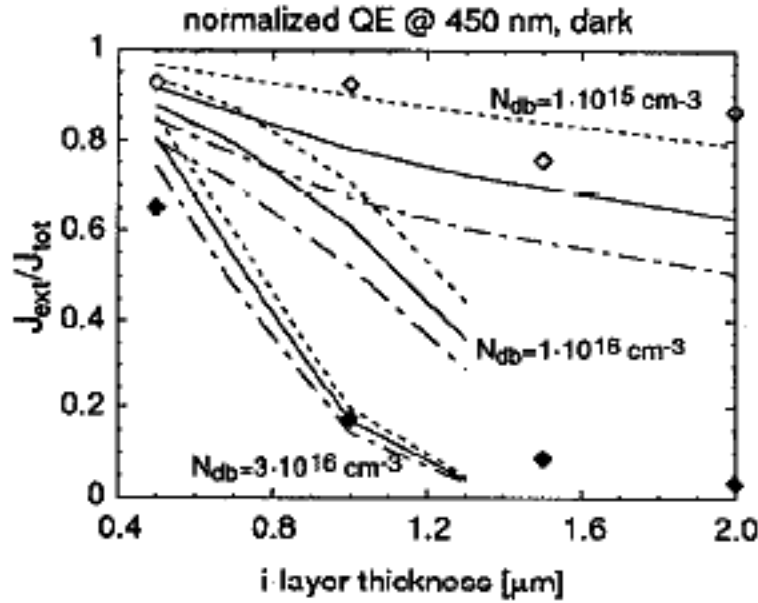


Figure 2: Normalized dark short wavelength QE at 450 nm: Experimental (symbols) and numerically computed (lines) data. The open symbols represent the annealed state, the full symbols the degraded state. The numbers indicate the bulk defect densities for each set of interface recombinations; the dashed, the full and the dotted-dashed lines correspond to interface recombination velocities of $3 \cdot 10^4 \text{ cm s}^{-1}$, $1 \cdot 10^5 \text{ cm s}^{-1}$, and $3 \cdot 10^5 \text{ cm s}^{-1}$, respectively.

thickness range. After the light-soaking, the QE_{450} shows a steep decrease for i -layers ranging from 0.5 to 1 μm , reaching values close to zero for larger thicknesses. The lines in Figure 2 represent the results of the numerical modelling. The modelling parameters are given in Table I. The parameters varied for the present work include the number of mid-gap defects (N_{DB}) in the bulk, and the interface recombination velocity for the electrons at the p - i interface (S_{p-i}). Whereas the defect density N_{DB} controls the bulk recombination rate, the interface recombination velocity controls the recombination rate at the p - i interface. The representation of the interface by a single recombination velocity is a first order approximation that for the present work yields equivalent results to the in depth models that include a microscopic description of interface states. The use of an interface recombination velocity also has the advantage of greatly reducing the number of modelling parameters.

As a result of the modelling it is obvious that by only increasing the bulk defect density the effect of the light-soaking on the QE_{450} as a function of the solar cell thickness is easily reproduced. On the other hand, changing interface recombination alone can not reproduce the observed experimental light-soaking behavior: increasing interface recombination leads to QE_{450} losses which are almost independent of the solar cell thickness (parallel shift of the curves). This result strongly supports the model that bulk defects produce the primary light-soaking effects in p - i - n solar cells. Figure 2 also shows that by measuring a set of cells in the i -layer thickness range where the QE_{450} is most sensitive to the bulk defects, one can get a good measure of the actual defect concentration. For standard device quality materials the range of sensitivity ranges from 0.3 to 1 μm . For larger thicknesses the QE_{450} after the light-soaking becomes too close zero to yield useful information.

In Figure 3 the modelled QE_{450} and the two loss components, interface loss and bulk loss, are shown as a function of bulk defect concentration. The interface

recombination velocity (S_{p-i}) is constant. Interestingly, the drop of the QE_{450} is a linear function of the bulk defect concentration over a wide range of defect concentrations,

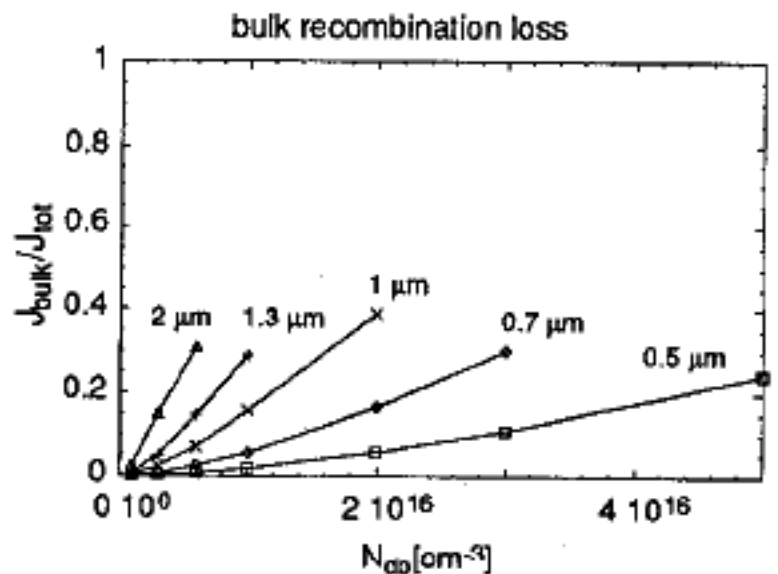
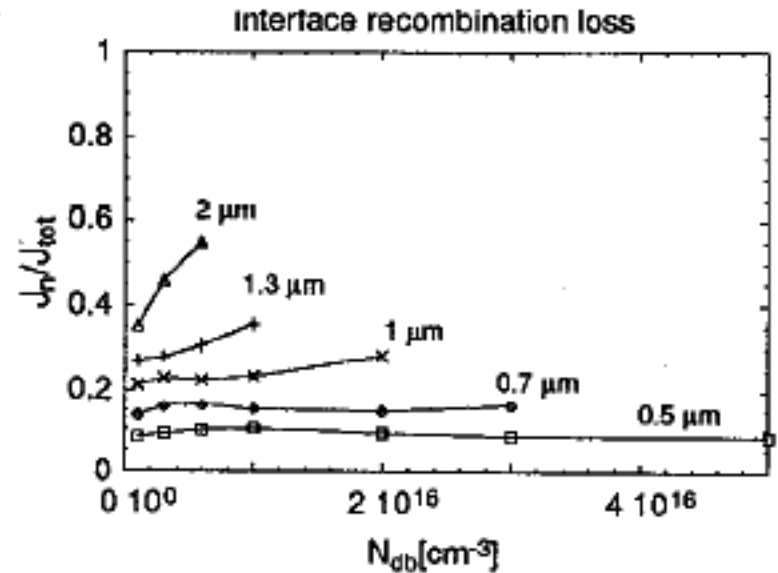
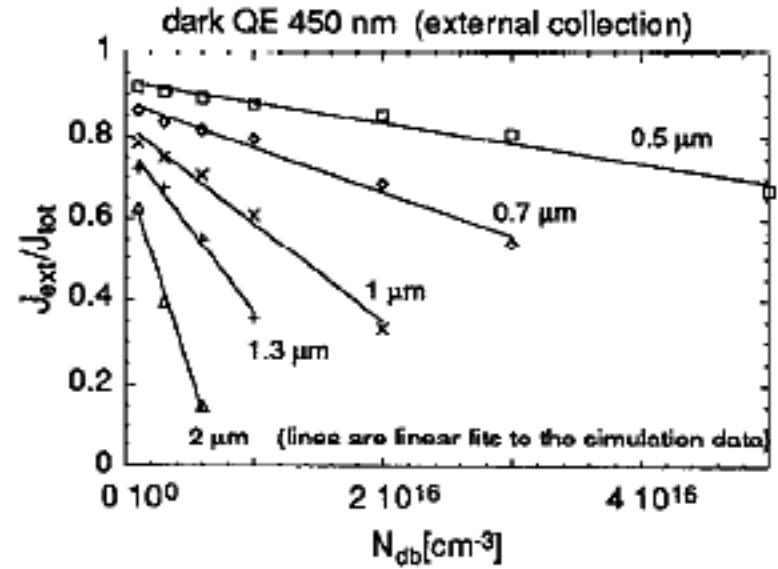


Figure 3: Numerically modelled normalized dark QE at 450 nm (QE_{450}), and its loss fraction due to interface recombination and its loss fraction due to bulk recombination, as a function of bulk defect density, and for i -layer thicknesses. The p -interface recombination velocity S_{p-i} is 10^5 cm s^{-1} .

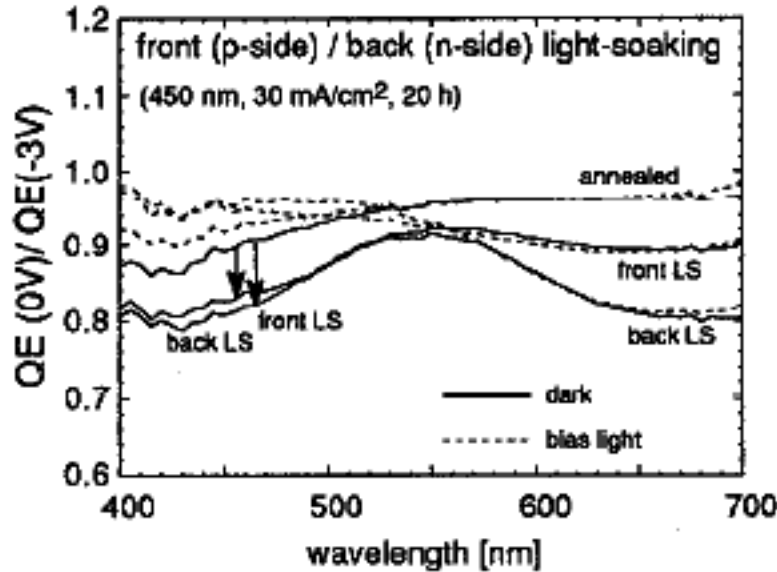


Figure 4: Normalized QE in the dark and with bias-light for a $0.5 \mu\text{m}$ thick solar cell as a function of front or back (through transparent back contact) light-soaking with strongly absorbed light (450 nm)

with different slopes for the different solar cell thicknesses (Figure 3a). By monitoring the decay of the QE_{450} , one can therefore directly track the increase of the bulk defects during the light-soaking. From the plots of the loss components it can be seen that the reduction of the QE_{450} is mainly due to an increase of recombination in the bulk, i.e. that holes diffuse back from the interface to recombine with accumulated electrons (Figure 3c). The other loss component, the back-diffusion of electrons to the p-i interface (Figure 3b), is found to be virtually constant for different defect densities (except for very thick devices).

Since the processes described above are located near the p-i interface it is reasonable to wonder how dangling bonds in other parts of the solar cell (e.g. near the n-i interface) affect the measurement. To determine the sensitivity of the measurement to other than uniform defect distributions in the i-layer, p-i-n solar cells were degraded with strongly absorbed light from either p-side or n-side. It was found that for the same dose of light-soaking, both front and back light-soaking lead to the same drop in QE_{450} (Figure 4). Numerical modelling of non-uniform defect profiles shows that this results from a twofold contribution of the bulk defects to the drop in QE_{450} . On the one hand, the negative charging of the defects at the n-side of the i-layer very efficiently reduces the electric field near the p-i interface, promoting the accumulation of the electrons and back diffusion of the holes. On the other hand, defects located near the p-i interface contribute directly to recombination losses as well as, to a lesser degree, to the field reduction. Given the result of the bifacial light-soaking, defects in both regions seem to have a similar efficiency in reducing the QE_{450} , thus the amplitude of the QE_{450} loss can be regarded as an integrated effect with defects from all parts of the solar cell i-layer contributing.

Figure 5 shows the QE data for two solar cells with relatively thick i-layers ($0.7 \mu\text{m}$). One cell was prepared with a low temperature i-layer ($T_{\text{sub}}=150^\circ\text{C}$) while the other cell was prepared with a standard i-layer ($T_{\text{sub}}=220^\circ\text{C}$). Both cells are measured in the annealed state, and after 120 hours of one sun light-soaking. From the short wavelength QE it is readily apparent that the cell with the low temperature i-layer has a higher defect concentration in the i-layer after light-

soaking, even though the annealed state behavior of both cells is nearly the same (see Figures 5 and 6). The high defect density after light-soaking then translates, as expected, to a greatly reduced degraded state efficiency in the low temperature solar cell, as seen in Figure 6.

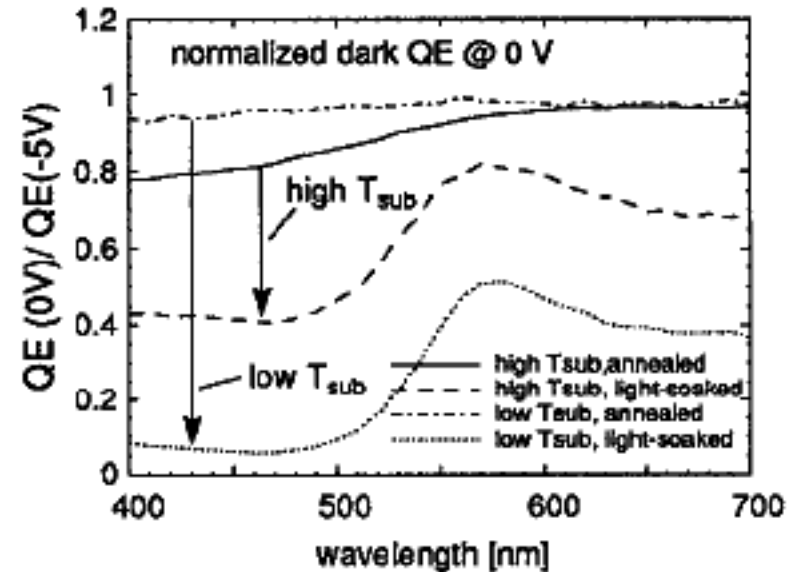


Figure 5: Normalized dark QE of p-i-n solar cells deposited at high (220°C) and low (150°C) substrate temperature, in the annealed state, and after 120 hours of light-soaking. The i-layer thickness is $0.7 \mu\text{m}$ in both cases.

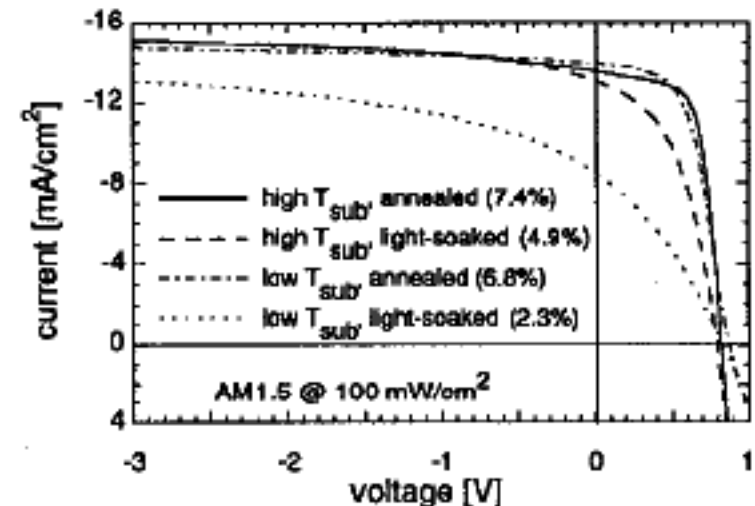


Figure 6: JV of p-i-n solar cells deposited at high (220°C) and low (150°C) substrate temperature, in the annealed state, and after 120 hours of light-soaking. Efficiency data is given in the legend. The i-layer thickness is $0.7 \mu\text{m}$ in both cases.

One possible explanation for the lack of stability in solar cells fabricated with low substrate temperature i-layers results from the low electron mobility we expect in i-layers grown at low substrate temperatures. Low electron mobility materials induce larger i-layer electron concentrations in illuminated solar cells.

In Figure 7 the increased electron concentration resulting from a factor of ten reduction in the electron mobility is seen. Therefore, if the defect generation rate scales with the n-p product of carrier concentrations, we expect, when all other factors are equal, that materials with low mobilities will degrade faster. Note, the stability model which relates the recombination rate to the defect concentration would not predict these observations as the recombination rate is not a function of the electron mobility.

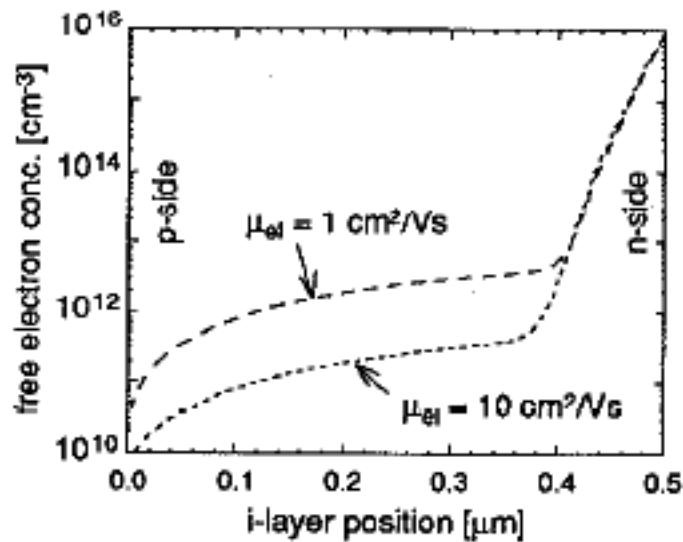


Figure 7: Numerically modeled free electron concentration as a function of i-layer position for different electron mobilities. The generation rate is $2 \cdot 10^{21} \text{ cm}^{-3} \text{ s}^{-1}$, the external voltage is 0V.

CONCLUSIONS

The manner in which material parameters interact with device parameters in amorphous silicon p-i-n solar cells is extremely intricate as mobilities, lifetimes, and field distributions all play a role in the observed performance of the solar cell. Fortunately, there are some simple solar cell measurements that help define the properties of the materials used to fabricate the i-layer of the solar cell. The short wavelength quantum efficiency measurement was shown to reveal the net density of charged and uncharged dangling bonds in the i-layer. The utility of this measurement was demonstrated by analysing the relative stability of solar cell prepared at different i-layer deposition temperatures. The results are consistent with an increased defect generation rate in the solar cell employing the low temperature i-layer. These results are similar to the decreased stability found on materials grown at faster deposition rates which not surprisingly have similar micro-structure.

The measurements and analysis presented here are helping to understand, evaluate, and assimilate various defect models, film measurements and material parameters into a single model which will help predict the stabilized efficiency of amorphous silicon solar cells. For example, thus far we have shown that the decreased stability trend seen in solar cells with low temperature i-layers is consistent with the larger carrier concentrations under operating conditions that result from the expected poor electron mobility in these materials.

ACKNOWLEDGEMENTS

The authors wish to thank S. Dubail for the sample preparation, and N. Pellaton for providing a low temperature sample. This work was supported by the Swiss Federal Office of Energy (OFEN) under contract EF-REN 90(045).

REFERENCES

- [1]: R. Street, to be published in *Mat.Res.Soc.Symp.Rec* (Spring 1993)
- [2]: T. X. Zhou et al, *Mat.Res.Soc.Symp.Rec* **219** (1991) p.451
- [3]: C. M. Fortmann et al, *J. Appl. Phys.* **64**(8)1988 p.4219
- [4]: J. Hou et al, *Proc. of 11th EC Photovoltaic Solar Energy Conference* (1992) p.750
- [5]: Y. Kuwano et al, *AIP Conference Proc.* **157** (1987) p.126
- [6]: C. M. Fortmann et al, *AIP Conference Proc.* **157** (1987) p.103
- [7]: C. R. Wronski et al, *Proc. of 11th EC Photovoltaic Solar Energy Conference*, (1992) p.72
- [8]: R. Dawson et al, to be published in *Appl. Phys. Letters*
- [9]: C. M. Fortmann and D. Fischer, to be published in *Appl.Phys. Letters*
- [10]: C. M. Fortmann et al, *J. of Non-Crystalline Solids*, **137&138** (1991) p.207
- [11]: D. Fischer et al, *Proc. of 11th EC Photovoltaic Solar Energy Conference* (1992) p.560
- [12]: W. Kusian and H. Pfeleiderer, *AIP Conference Proc.* **234** (1991) p.290
- [13]: F. Smole and J. Furlan, *Proc. of 11th EC Photovoltaic Solar Energy Conference*, (1992) p.765